Article:

Zhang, K. and Gubbins, D. (2000) Scale disparities and magnetohydrodynamics in the Earth's core. Philosophical Transactions Of The Royal Society Of London Series A - Mathematical Physical and Engineering Sciences, 358 (1768). pp. 899-920. ISSN: 1471-2962

https://doi.org/10.1098/rsta.2000.0566

THE ROYAL SOCIETY

Scale disparities and magnetohydrodynamics in the Earth's core

By Keke Zhang[1] and David Gubbins[2]

[1]*School of Mathematical Sciences, University of Exeter, Exeter EX4 4QJ, UK*
[2]*School of Earth Sciences, University of Leeds, Leeds LS2 9JT, UK*

Fluid motions driven by convection in the Earth's fluid core sustain geomagnetic fields by magnetohydrodynamic dynamo processes. The dynamics of the core is critically influenced by the combined effects of rotation and magnetic fields. This paper attempts to illustrate the scale-related difficulties in modelling a convection-driven geodynamo by studying both linear and nonlinear convection in the presence of imposed toroidal and poloidal fields. We show that there exist three extremely large disparities, as a direct consequence of small viscosity and rapid rotation of the Earth's fluid core, in the spatial, temporal and amplitude scales of a convection-driven geodynamo. We also show that the structure and strength of convective motions, and, hence, the relevant dynamo action, are extremely sensitive to the intricate dynamical balance between the viscous, Coriolis and Lorentz forces; similarly, the structure and strength of the magnetic field generated by the dynamo process can depend very sensitively on the fluid flow. We suggest, therefore, that the zero Ekman number limit is strongly singular and that a stable convection-driven strong-field geodynamo satisfying Taylor's constraint may not exist. Instead, the geodynamo may vacillate between a strong field state, as at present, and a weak field state, which is also unstable because it fails to convect sufficient heat.

Keywords: geodynamo; Taylor constraint; Earth's core; magnetoconvection

1. Introduction

The primary dynamics of the Earth's fluid core is controlled by (1) rapid rotation, (2) small viscosity, (3) thermal or compositional convection, and (4) a self-generated magnetic field (Moffatt 1978; Busse 1978; Gubbins & Roberts 1987; Roberts & Soward 1992; Hollerbach 1996; Fearn 1997). Other details such as compressibility, variable rotation, boundary conditions, or the origin of buoyancy (thermal or compositional) are of secondary importance to the dynamics on the long (magnetic-diffusion) time-scale, for which the Coriolis force must be balanced primarily by four forces,

$$2\boldsymbol{\Omega} \times \mathbf{u} = -\frac{1}{\rho}\nabla p + \alpha\Theta g_0\mathbf{r} + \frac{1}{\rho\mu}(\nabla \times \mathbf{B}) \times \mathbf{B} + \nu\nabla^2\mathbf{u}, \tag{1.1}$$

where $\mathbf{r}$ is the position vector, ρ the mean density of the Earth's liquid core, g_0 the acceleration of gravity, $\boldsymbol{\Omega}$ the angular velocity of the Earth, Θ the deviation of temperature from the adiabatic, ν the kinematic viscosity, μ the magnetic permeability, α the thermal expansion coefficient, $\mathbf{u}$ the velocity field, and $\mathbf{B}$ the generated magnetic field. In equation (1.1), $2\boldsymbol{\Omega} \times \mathbf{u}$ is the Coriolis force, $-(\nabla p)/\rho$ the pressure force, $\alpha\Theta g_0\mathbf{r}$ the buoyancy force, $(\nabla \times \mathbf{B}) \times \mathbf{B}/\rho\mu$ the magnetic (Lorentz) force, and $\nu\nabla^2\mathbf{u}$ the viscous force. The inertial force $(\partial\mathbf{u}/\partial t + \mathbf{u}\cdot\nabla\mathbf{u})$ has been neglected because its contribution on the magnetic diffusion time-scale is small. On the shorter, century-long, advection time-scale, however, inertia may play an important role in providing an extra way to relax the rotational constraint or for a dynamo solution to remain close to the Taylor constraint (see equation (1.2) below). The centrifugal force, $\rho\boldsymbol{\Omega} \times (\boldsymbol{\Omega} \times \mathbf{r})$, has been absorbed into the modified pressure, p.

The small viscosity makes equation (1.1) very difficult to treat, and two different approaches have been developed to solve it. The first assumes that the zero viscosity limit, $\nu \to 0$, is non-singular. Setting $\nu = 0$, integrating the $\hat{\phi}$-component of (1.1) over the surface of a geostrophic cylinder $G(s)$ with radius s and axis parallel to that of rotation, and using the incompressibility condition $\nabla\cdot\mathbf{u} = 0$, gives Taylor's constraint (Taylor 1963; see also Jault 1995; Fearn 1998; Walker & Hollerbach 1999):

$$\int_{G(s)} [(\nabla \times \mathbf{B}) \times \mathbf{B}]_\phi \, \mathrm{d}S = 0. \tag{1.2}$$

The magnetic field must satisfy Taylor's constraint for (1.1) to hold without viscosity; if such a solution exists it is called a *strong-field* dynamo. There have been many attempts to obtain a convection-driven strong-field dynamo where viscosity plays at most a minor role in boundary layers (see, for example, Fearn & Proctor 1987; Walker *et al.* 1998), but all have failed.

The second approach is to replace the small viscosity of the Earth's core by a much larger one, sometimes with an artificial form of hyperviscosity in which small length-scales see a higher effective viscosity. This has resulted in considerable progress (see, for example, Glatzmaier & Roberts 1995*a*, *b*, 1996*a*, *b*; Kuang & Bloxham 1997; Jones *et al.* 1995; Sarson & Jones 1999). The resulting dynamos are able to generate magnetic fields and flows of the right strength and morphology to model the Earth; they also have the potential to explain geomagnetic reversals. However, they are in the wrong regime for the Earth, with viscous forces playing a significant dynamical role. This makes comparing the numerical simulations with observations hazardous: an Earth-like polarity reversal may appeal, but we learn little about the Earth if the force balance in the model fails to match that in the core.

At first glance, the strong-field dynamo presents the most attractive model of magnetohydrodynamics in the Earth's core: it has a large-scale convective flow, a strong toroidal magnetic field, nearly negligible viscous dissipation, and an efficient thermal dynamo engine. In practice, such dynamos fail in a number of ways (see, for example, Fearn 1998), most instructively, when the dynamo equations are integrated in time starting from initial conditions provided by a magnetoconvection calculation. In magnetoconvection, the field is imposed; once time integration starts, the imposed field is removed, leaving only that generated by the dynamo process. One of us (K.Z.) has conducted a number of such numerical experiments with similar results. The strength of the initial magnetic field gradually decreases over a few magnetic diffusion times and, at the same time, small-scale convective motions become dominant. Dynamo action subsequently collapses completely because the amplitude of convection drops below the critical value; sometimes even the convection shuts off because the Rayleigh number falls below the critical value. Increasing the viscosity, or introducing hyperdiffusivity, prevents this collapse because the additional viscosity prevents dominance of small-scale convection at times when the field is weak. The artificially high viscosity is, therefore, responsible for sustaining the dynamo action, hardly what we imagine happening in the core.

The first aim of numerical modelling is not to reproduce exactly the right values of the parameters in the core, but to approach the correct dynamical regime. We have so far been unable to do this for the geodynamo because of the small viscosity, yet magnetoconvection calculations can be extrapolated to very small viscosity quite realistically. Why is the dynamo calculation so very much more difficult than magnetoconvection with the same imposed parameters? We argue here that it is because the self-generated field strength can vary, leading to huge ranges of time-, length- and amplitude scales that are very hard to deal with numerically. The problems at small Ekman number are, therefore, much more subtle than simply resolving boundary layers or achieving exactly the right scales for the Earth.

We suggest here that the strong-field dynamo is in fact unstable and prone to collapse into a weak-field state similar to non-magnetic convection. The argument is based on results from magnetoconvection extrapolated to the very small values of viscosity found in the core; it receives some support from recent palaeomagnetic evidence that the Earth's magnetic field collapses and almost reverses many times between full polarity reversals (Gubbins 1999), and that its amplitude varies dramatically on a millennium time-scale (see, for example, Channel, this issue).

2. Mathematical formulation

To a first approximation, the dynamics of the Earth's liquid core is governed by the following equations of motion, heat and induction in a spherical shell of electrically conducting Boussinesq fluid with inner radius r_{i} and outer radius r_{o}:

$$\frac{\partial \mathbf{u}}{\partial t} + \mathbf{u}\cdot\nabla\mathbf{u} + 2\Omega\mathbf{k}\times\mathbf{u} = -\frac{1}{\rho}\nabla p + \alpha\Theta g_0\mathbf{r} + \frac{1}{\rho\mu}(\nabla\times\mathbf{B})\times\mathbf{B} + \nu\nabla^2\mathbf{u}, \tag{2.1}$$

$$\frac{\partial \Theta}{\partial t} + \mathbf{u}\cdot\nabla\Theta + \mathbf{u}\cdot\nabla T_{\mathrm{s}} = \kappa\nabla^2\Theta, \tag{2.2}$$

$$\frac{\partial}{\partial t}\mathbf{B} + \mathbf{u}\cdot\nabla\mathbf{B} = \mathbf{B}\cdot\nabla\mathbf{u} + \lambda\nabla^2\mathbf{B}, \tag{2.3}$$

where $\mathbf{k}$ is a unit vector parallel to the axis of rotation, $T_{\mathrm{s}} = \beta r^2/2$ is a basic unstable temperature produced by the uniform distribution of heat sources (Chandrasekhar 1961; Roberts 1968), and t is time.

Equations (2.1)–(2.3) can be non-dimensionalized as follows:

$$r \to dr, \qquad t \to td^2/\kappa, \qquad \Theta \to \Theta\beta d^2, \qquad \mathbf{b} \to B_0\mathbf{b}, \tag{2.4}$$

where $d = (r_{\mathrm{o}} - r_{\mathrm{i}})$ and B_0 is a typical amplitude of the generated magnetic field. In dimensionless form, the governing equations become

$$EPr^{-1}\left|\frac{\partial \mathbf{u}}{\partial t} + \mathbf{u}\cdot\nabla\mathbf{u}\right| + \mathbf{k}\times\mathbf{u} = -\nabla p + RE\Theta\mathbf{r} + \Lambda(\nabla\times\mathbf{B})\times\mathbf{B} + E\nabla^2\mathbf{u}, \tag{2.5}$$

$$\left|\nabla^2 - \frac{\partial}{\partial t}\right| \; \Theta = \mathbf{u}\cdot\nabla\Theta - \mathbf{r}\cdot\mathbf{u}, \tag{2.6}$$

$$\left|\nabla^2 - \frac{\partial}{\partial t}\right| \; \mathbf{B} = R_{\mathrm{m}}(\mathbf{u}\cdot\nabla\mathbf{B} - \mathbf{B}\cdot\nabla\mathbf{u}). \tag{2.7}$$

The Rayleigh number R, Ekman number E, Elsasser number Λ, and magnetic Reynolds number R_{m} are defined, respectively, as

$$R = \frac{\alpha\beta g_0 d^4}{\nu\kappa}, \qquad E = \frac{\nu}{2\Omega d^2}, \qquad \Lambda = \frac{B_0^2}{2\Omega\mu\rho\lambda}, \qquad R_{\mathrm{m}} = \frac{\mathcal{U}d}{\lambda}, \tag{2.8}$$

where $\mathcal{U}$ is a typical amplitude of the convection-driven flow.

Consider solutions for the magnetoconvection problem, in which a magnetic field is imposed on the system. In magnetoconvection, the Elsasser number Λ is determined by the strength of the imposed magnetic field, whereas for the full dynamo problem, the magnetic field is self-generated and its typical strength is determined by the solution. The Elsasser number could, therefore, be dispensed with (by setting $B_0 = \sqrt{2\Omega\mu\rho\lambda}$) in the dynamo problem, but this is not helpful for magnetoconvection because we wish to study the response of the system to different amplitudes of the imposed magnetic field.

Next, consider solutions to the kinematic dynamo problem, in which the fluid velocity is imposed. The magnetic Reynolds number R_{m} is determined by the strength of the imposed velocity, whereas for the full dynamo problem it is determined by the solution. In the kinematic dynamo problem, we wish to determine the flow speed required to generate magnetic field, making R_{m} the important external parameter, but, like the Elsasser number, it can be dispensed with for the full dynamo problem. With the scaling for the velocity used to form the dimensionless equation of motion (2.5), the flow strength is $\mathcal{U} = \kappa/d$ and the magnetic Reynolds number (2.8) becomes the Roberts number,

$$R_{\mathrm{m}} = \kappa/\lambda = q, \tag{2.9}$$

a property of the fluid.

The kinematic dynamo and magnetoconvection are parallel simplifications of the full dynamo problem: in the first, $\mathbf{u}$ is fixed and (2.3) is solved for $\mathbf{B}$, whereas in the second, $\mathbf{B}$ is fixed and (2.1)–(2.2) are solved for $\mathbf{u}$. Both problems can be expected to reveal some of the character of the full dynamo problem, but they differ from each other in important respects. The kinematic problem linearizes equation (2.3) (in $\mathbf{B}$), yet it remains the correct equation for the full dynamo, whose solution must still satisfy (2.3). Equations (2.1)–(2.2) remain nonlinear even when $\mathbf{B}$ is fixed; many of the results quoted are for marginal or weakly nonlinear convection in which the flow is weak and the nonlinear terms small. No such restriction applies to the kinematic dynamo problem.

In this paper, we simplify the equations further by taking the Roberts number to be unity and the Prandtl number to be infinite:

$$q = \frac{\kappa}{\lambda} = 1, \qquad Pr = \frac{\nu}{\kappa} = \infty. \tag{2.10}$$

Neither choice applies to the core directly, but we justify the first because turbulence is expected to act to equalize the diffusivities and the second because small Prandtl number flow is characterized by rapid time variations that are not observed in the geomagnetic record. We set $\eta = r_{\mathrm{i}}/r_{\mathrm{o}} = 0.4$ for our analysis throughout the paper.

The buoyancy-driven magnetohydrodynamic problem involves solving equations (2.5)–(2.7) and

$$\nabla \cdot \mathbf{u} = 0, \tag{2.11 a}$$

$$\nabla \cdot \mathbf{B} = 0, \tag{2.11 b}$$

together with appropriate boundary conditions for $\mathbf{u}$, $\mathbf{B}$ and Θ. We assume that the inner and outer bounding spherical surfaces of the Earth's core are stress free and impenetrable,

$$\frac{\partial(u_\phi/r)}{\partial r} = \frac{\partial(u_\theta/r)}{\partial r} = u_r = 0, \tag{2.12}$$

where (u_r, u_θ, u_ϕ) are the components of velocity in spherical polar coordinates. Stress-free conditions give weaker boundary layers than rigid boundary conditions: note that the type of the velocity boundary condition does not make a leading-order contribution when E is sufficiently small (Roberts 1965; Zhang & Jones 1993; Fearn 1979). We also assume that both inner core and mantle are perfectly electrically insulating and thermally conducting, which yields

$$\mathbf{r} \cdot (\nabla \times \mathbf{B}) = \Theta = 0, \qquad [\mathbf{B}] = 0, \tag{2.13}$$

on the inner and outer bounding spherical surfaces, where $[\cdot]$ denotes the jump across the bounding surfaces. This model does not include the potential stabilizing effect of an electrically conducting inner core (Hollerbach & Jones 1993, 1995). The numerical methods employed are described in Gubbins & Zhang (1993), Gubbins *et al.* (2000*a*), and papers cited therein.

In order to provide an example of the scaling disparities, we have solved four different related convection problems in this paper for various values of E, R and Λ: the problems of linear and nonlinear convection with $\Lambda = 0$ governed by equations (2.5), (2.6) and (2.11 *a*); and the problems of linear and nonlinear convection in the presence of an imposed magnetic field governed by equations (2.5)–(2.7), (2.11 *a*) and (2.11 *b*). We also use solutions to the kinematic problem obtained by solving (2.7) with a parametrized flow containing some of the characteristics of core convection to illustrate the variation in flow speed required to generate magnetic field from flows with slightly different forms.

3. Spatial, temporal and amplitude scales with a weak field

When the dynamic effect of a magnetic field is sufficiently small, the Lorentz force may be neglected, decoupling the equations of motion and induction. There are then two fundamentally different types of convection. The first takes the form of thermal inertial waves, which oscillate so fast that viscosity may be neglected to leading order to give the Poincaré equation in a rotating spherical system (Zhang 1994, 1995*b*). Viscosity usually plays a purely dissipative role and the limit $E \to 0$ is regular. Only at the next order of approximation does the buoyancy force maintain convection against weak viscous dissipation, which takes place in Ekman boundary layers. However, this type of convection, which is associated with small Prandtl number, is unlikely to be important or relevant to dynamo action in the Earth's core simply because of the short time-scale of the convective flow.

We shall focus on the second form of convection (Roberts 1968; Busse 1970; see also Jones *et al.* 2000), associated with large Prandtl number. It is slowly oscillatory and the inertial terms do not enter into the leading-order problem. The most significant feature of the convection is the role of viscosity: it provides the necessary frictional forces to offset that part of the Coriolis force $2\Omega\mathbf{k} \times \mathbf{u}$ that cannot be balanced by the pressure gradient $-\nabla p/\rho$. Convection cannot take place without a large frictional force; in this sense, the role of viscosity is inverted from the usual one of inhibiting or preventing convection (by providing a sink for potential energy that would otherwise be converted to kinetic energy), to an essential force that allows convection to occur by breaking the Proudman–Taylor constraint imposed by the rotation.

Application of the operator $\mathbf{r} \cdot \nabla\times$ to (2.5) yields the radial component of the vorticity equation

$$-\mathbf{r} \cdot \frac{\partial \mathbf{u}}{\partial z} = E\mathbf{r} \cdot \nabla \times \nabla \times \nabla \times \mathbf{u}, \tag{3.1}$$

where (s, ϕ, z) are cylindrical polar coordinates with z along $\mathbf{k}$. The Proudman–Taylor theorem requires changes of $\mathbf{u}$ and Θ to be small at low viscosity, so that $\partial/\partial z$ is $O(1)$. The primary balance in the equation of motion is between pressure and Coriolis forces, but in the vorticity equation there is no pressure and the balance must be struck with the viscous forces. This is achieved at small Ekman number by small length-scales in the s and ϕ directions. $(\nabla\times)^3$ may be taken to be $O(m^3)$, where m is the azimuthal wavenumber of convection. Equation (3.1) shows that the limit $E \to 0$ is singular because the wavelength of the convective flow goes to zero:

$$m = O\left[\left|\frac{\nu}{2\Omega d^2}\right|^{-1/3} \right] = O(E^{-1/3}), \quad \text{as } E \to 0. \tag{3.2}$$

Equation (3.2) is one of the fundamental asymptotic laws that provide a basic framework for understanding convection in a sphere.

Note that equations (3.1) and (3.2) are valid at infinite Prandtl number regardless of the size of the Rayleigh number R. Thus, provided no small scales develop in the z-direction, the presence of large wavenumbers (small scales) will persist even in a strongly nonlinear regime. The fundamental laws were first derived by Roberts (1968) from his asymptotic theory for a rapidly rotating sphere,

$$R_{\mathrm{c}} = O(E^{-4/3}), \quad m_{\mathrm{c}} = O(E^{-1/3}), \quad \omega_{\mathrm{c}} = O(E^{-2/3}), \quad \text{as } E \to 0, \tag{3.3}$$

where R_{c} is the critical Rayleigh number, the smallest value of the Rayleigh number at which convection can take place, and m_{c} and ω_{c} are the corresponding wavenumber and frequency of convection (see also Soward 1977; Zhang 1991, 1992; Jones *et al.* 2000).

In (3.3), the coefficients of the asymptotic laws are functions of the Prandtl number Pr. It was shown by Busse (1970), based on a local asymptotic analysis, that convection with symmetry

$$(u_r, u_\theta, u_\phi)(r, \theta, \phi) = (u_r, -u_\theta, u_\phi)(r, \pi - \theta, \phi), \qquad \Theta(r, \theta, \phi) = \Theta(r, \pi - \theta, \phi), \tag{3.4}$$

Table 1. *An example of the scale disparities for* $E = 10^{-5}$

(The critical Rayleigh number R_c, the corresponding azimuthal wavenumber m_c and the frequency ω_c of convection in a rapidly rotating spherical shell with or without the effect of a magnetic field for $r_i/r_o = 0.4$. The parameter ϵ_P is related to the form of the basic magnetic field in the magnetoconvection problem defined by (4.1). The time-scale of the frequency is based on the magnetic diffusion time-scale with $q = 1$.)

Pr, q	R_c	ω_c	m_c	Λ	ϵ_P
1 , 1	$+7.52 \times 10^6$	$-923.$	36	0.0	0
1 , 1	$+9.59 \times 10^5$	$+0.18$	2	8.0	0
1 , 1	$+1.14 \times 10^6$	$+8.01$	1	10	0
1 , 1	-1.54×10^6	-0.45	1	10	0.17

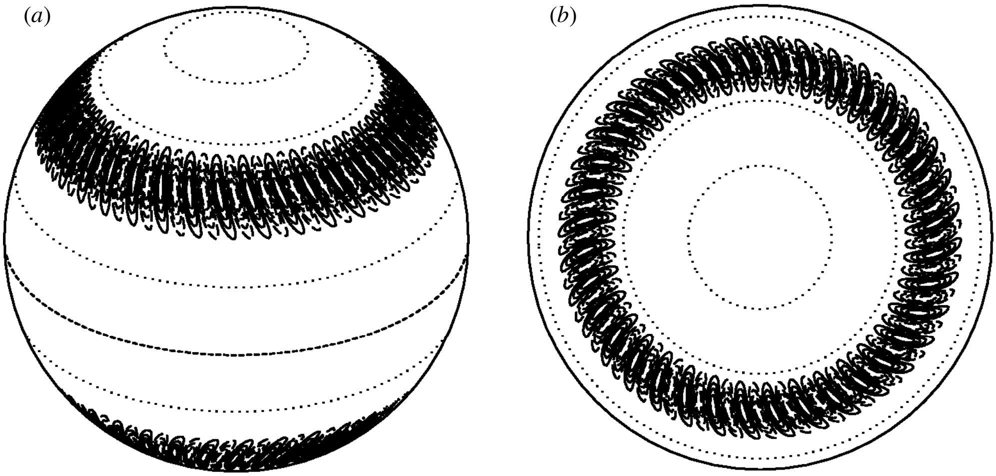

Figure 1. The small spatial scale and short time-scale convection in a rapidly rotating spherical fluid shell with $r_i/r_o = 0.4$ at $E = 10^{-5}$ with no magnetic field ($\Lambda = 0$, see also table 1). Shown are streamlines of the convective flow on the outer spherical surface viewed from a 30° angle (*a*) and viewed from the North Pole (*b*).

occurs at lowest R_c and is, therefore, physically realizable. The multiplicative constants in these asymptotic laws can be found by extrapolating the results of numerical calculations with finite E. For a rotating spherical shell with $r_i/r_o = 0.4$ they are

$$R_c = 1.63E^{-4/3}, \quad m_c = 0.74E^{-1/3}, \quad \omega_c = -0.25E^{-2/3}, \quad \text{as } E \to 0. \qquad (3.5)$$

An example of the convection solution at $E = 10^{-5}$, which shows streamlines on the outer spherical surface, is displayed in figure 1. More details are given in table 1. These solutions are new, although their behaviour was already qualitatively well understood: they were computed for this paper in order to establish the asymptotic behaviour at small E. The convection is in the form of nearly two-dimensional rolls (Busse's columnar rolls) aligned with the axis of rotation and located and localized at higher latitudes with a weak phase shift.

Nonlinear calculations have been performed to obtain the corresponding weakly nonlinear asymptotic law for the amplitude of convection, which is

$$\mathcal{U} = 20.1(RE^{4/3} - 1.63)^{1/2}\lambda/d, \tag{3.6}$$

where $\mathcal{U}$ is now defined precisely as the average speed of convection over the spherical fluid shell V:

$$\mathcal{U}^2 = \int_V |\mathbf{u}|^2\,\mathrm{d}V \;\Big/ \int_V \mathrm{d}V. \tag{3.7}$$

We know the approximate flow speed in the Earth's core, so it is useful to rearrange (3.6) to give the corresponding Rayleigh number:

$$R_U = \left[\left(\frac{\mathcal{U}d}{20.1\lambda}\right)^2 + 1.63\right]E^{-4/3}. \tag{3.8}$$

The corresponding dominant wavenumber and frequency are only slightly modified by the nonlinearity. Similarly, a weakly nonlinear asymptotic relation for the total convective heat flux H at the outer spherical surface can also be obtained

$$H = (4\pi r_0^2 K_\mathrm{T})\frac{\Delta T}{d}3.72 \times 10^{-2}(RE^{4/3} - 1.63), \tag{3.9}$$

where K_T is the thermal conductivity, and ΔT is the superadiabatic temperature difference across the fluid shell.

These asymptotic laws can be used to extrapolate the results to low Ekman number, when the length-scales are much too small to be simulated numerically. Molecular diffusivities ($\nu = \kappa = 10^{-6}$ m^2 s^{-1}) give $E \approx 10^{-15}$ in the Earth's core, turbulent values ($\nu = \kappa = \lambda$) give $E \approx 10^{-10}$. Taking $d = 2 \times 10^6$ m and $\lambda = 1$ m^2 s^{-1} ($q = 1$) we obtain for $E = 10^{-15}$

$$R_\mathrm{c} = 1.6 \times 10^{20}, \quad L = 27\,\mathrm{m}, \quad T = 10^4\,\mathrm{s}, \quad \text{for } E = 10^{-15}, \tag{3.10}$$

where L is the horizontal scale of convection rolls and T is the period of oscillation (or azimuthal drift), both of which are extremely small, and, for $E = 10^{-10}$,

$$R_\mathrm{c} = 3.5 \times 10^{13}, \quad L = 1.3\,\mathrm{km}, \quad T = 3.4 \times 10^6\,\mathrm{s}, \quad \text{for } E = 10^{-10}, \tag{3.11}$$

which still gives small-scale, rapidly fluctuating convection for core parameters.

If we further assume that the weakly nonlinear expressions (3.6), (3.9) remain valid for strongly nonlinear convection, we may estimate the size of the Rayleigh number and the convective heat flux. Taking a typical core flow speed estimated from geomagnetic secular variation to be $\mathcal{U} = 10^{-4}$ m s^{-1}, we can use equation (3.8) to estimate the Rayleigh number $R_U = 10^{22}$ for $E = 10^{-15}$ and $R_U = 2.2 \times 10^{15}$ for $E = 10^{-10}$. Note that in both cases the required Rayleigh number is 60 times critical, because both R and R_c scale with the same power of the Ekman number.

These numerical estimates are presented here to demonstrate the extremes of scale that arise in non-magnetic convection. Their relevance for the Earth's core is discussed in § 7; they are only given here for comparison with magnetoconvection and full dynamo calculations.

4. Spatial, temporal and amplitude scales with a strong toroidal field

We now assume the fluid is permeated by an axisymmetric magnetic field with both toroidal and poloidal parts:

$$\mathbf{B} = B_0(\epsilon_{\mathrm{P}}\mathbf{B}_{\mathrm{P}} + \mathbf{B}_{\mathrm{T}}), \tag{4.1}$$

where $\mathbf{B}_{\mathrm{T}}$ is the toroidal part and $\mathbf{B}_{\mathrm{P}}$ the poloidal part, scaled so that $|\mathbf{B}_{\mathrm{P}}|_{\max} = |\mathbf{B}_{\mathrm{T}}|_{\max} = 1$. Further, we assume that $\mathbf{B}$ has dipole symmetry (see, for example, Gubbins & Zhang 1993)

$$(B_r, B_\theta, B_\phi)(r, \theta, \phi) = (-B_r, B_\theta, -B_\phi)(r, \pi - \theta, \phi). \tag{4.2}$$

This imposed field is supposed to represent the main dynamo-generated field in the Earth's core, but the equations are only self-consistent if we suppose the field is maintained by some external source, because we are not solving the full dynamo equations. Any axisymmetric toroidal field $\mathbf{B}_{\mathrm{T}}$ can be written in the form

$$\mathbf{B}_{\mathrm{T}} = -\sum_{l,n} g_{ln} \frac{\partial G_{ln}(\theta, r)}{\partial \theta}\hat{\phi}, \tag{4.3}$$

where g_{ln} are real constants and $G_{ln}(\theta, r)$ are solutions of Helmholtz's equation

$$(\beta_{ln}^2 + \nabla^2)G_{ln}(\theta, r) = 0, \tag{4.4}$$

which have the form

$$G_{ln}(\theta, r) = P_l(\cos\theta)[j_l(r_{\mathrm{i}}\beta_{ln})n_l(r\beta_{ln}) - j_l(r\beta_{ln})n_l(r_{\mathrm{i}}\beta_{ln})], \tag{4.5}$$

where $P_l(\cos\theta)$ is the Legendre function, $j_l(r\beta_{ln})$ and $n_l(r\beta_{ln})$ are spherical Bessel functions of the first and second kinds, and the β_{ln} are determined by

$$j_l(r_{\mathrm{i}}\beta_{ln})n_l(r_{\mathrm{o}}\beta_{ln}) - j_l(r_{\mathrm{o}}\beta_{ln})n_l(r_{\mathrm{i}}\beta_{ln}) = 0, \tag{4.6}$$

with

$$0 < \beta_{l1} < \beta_{l2} < \beta_{l3} < \cdots, \quad l = 1, 2, 3, \ldots. \tag{4.7}$$

Similarly, any poloidal magnetic field $\mathbf{B}_{\mathrm{P}}$ may be written in the form

$$\mathbf{B}_{\mathrm{P}} = \sum_{l,n} h_{ln} \left[\left(-r\nabla^2 H_{ln} + \frac{1}{r}\frac{\partial}{\partial r} r^2 \frac{\partial H_{ln}}{\partial r} \right) \hat{\mathbf{r}} + \frac{1}{r}\frac{\partial}{\partial \theta}\frac{\partial(rH_{ln})}{\partial r}\hat{\boldsymbol{\theta}} \right], \tag{4.8}$$

where h_{ln} are real constants and $H_{ln}(\theta, r)$ satisfies

$$(\xi_{ln}^2 + \nabla^2)H_{ln}(\theta, r) = 0, \tag{4.9}$$

with ξ_{ln} being determined by

$$j_l(r_{\mathrm{i}}\xi_{ln})n_{l-1}(r_{\mathrm{o}}\xi_{ln}) - j_{l-1}(r_{\mathrm{o}}\xi_{ln})n_l(r_{\mathrm{i}}\xi_{ln}) = 0, \tag{4.10}$$

with $0 < \xi_{l1} < \xi_{l2} < \xi_{l3} < \cdots$. We mimic the geomagnetic field, which is dominated by the largest scales, by choosing $l = 1$, $n = 1$ for the poloidal field and $l = 2$, $n = 1$ for the toroidal field. The problem of magnetoconvection, although the magnetic

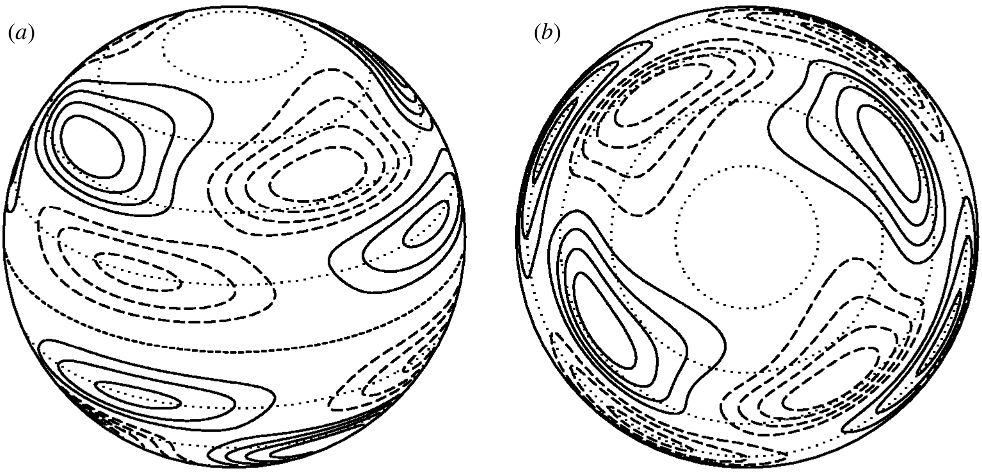

Figure 2. The large spatial scale and long time-scale convection in a rapidly rotating spherical fluid shell with $r_i/r_o = 0.4$ at $E = 10^{-5}$ with imposed toroidal magnetic field at $\Lambda = 8$, $\epsilon_P = 0$ (see also table 1). Views (*a*) and (*b*) as in figure 1.

field is imposed, contains many essential dynamic elements similar to those in magnetohydrodynamic dynamos (Proctor 1994; see also Fearn & Proctor 1983; Zhang & Jones 1994; Zhang 1995*a*; Olson & Glatzmaier 1995, 1996).

When a strong magnetic field is imposed onto the convection system *all the time*, the dynamical role of viscosity can be taken up by the magnetic force. This can easily be seen by taking the radial component of the vorticity equation from (2.5),

$$\mathbf{r} \cdot \frac{\partial \mathbf{u}}{\partial z} \sim \Lambda \mathbf{r} \cdot ((\nabla \times \mathbf{B}) \times \mathbf{B}). \tag{4.11}$$

Taking $\partial/\partial z = O(1)$ together with Ohm's law yields an estimate $L = O(d\bar{\Lambda})$, where $\bar{\Lambda}$ is the Elsasser number with B_0 based on an average magnetic field. For a sufficiently strong imposed field, $\bar{\Lambda} = O(1)$, the fundamental asymptotic laws for convection (3.3) are replaced by

$$R_c = O(E^{-1}), \quad m_c = O(\bar{\Lambda}^{-1}), \quad \omega_c = O(1), \quad \text{as } E \to 0. \tag{4.12}$$

The convection is large scale and slowly varying on the diffusion time-scale, in sharp contrast to non-magnetic convection (3.3). Furthermore, the Rayleigh number required to initiate convection is much smaller ($O(E^{-1})$, in contrast with $O(E^{-4/3})$ in (3.3), a factor of $E^{-1/3}$ or 10^5 for molecular values of the diffusivities).

Again, the asymptotic laws can be verified and values placed on the coefficients by numerical simulation at relatively large Ekman numbers. For a purely toroidal field with $\epsilon_P = 0$ and $\Lambda = 10$ (which is based on the maximum value of $|\mathbf{B}|$, equivalent to $\bar{\Lambda} = O(1)$), we obtain

$$R_c = 12E^{-1}, \quad m_c = 1, \quad \omega_c = -8.3, \quad \text{as } E \to 0, \tag{4.13}$$

which should be compared with (3.5). An example of our convection solution for $E = 10^{-5}$ and $\Lambda = 8$ is shown in figure 2. It displays streamlines of the convective motions on the outer spherical surface, which should be compared with figure 1 with $\Lambda = 0$. Details of the relevant parameters for figure 2 are also given in table 1.

Nonlinear calculations at $\epsilon_{\mathrm{P}} = 0$ (Zhang 1999) give the corresponding weakly nonlinear asymptotic relation for the finite amplitude of magnetoconvection corresponding to (3.6):

$$\mathcal{U} = 3(RE - 12)^{1/2}\lambda/d, \quad \text{as } E \to 0. \tag{4.14}$$

Similarly, the relation corresponding to (3.9) for the heat flux H is:

$$H = 1.01 \times 10^{-2}(4\pi r_{\mathrm{o}}^2 K_{\mathrm{T}})\Delta T(RE - 12)/d. \tag{4.15}$$

With both linear and nonlinear asymptotic relations for $E \to 0$, we can again estimate quantities in the Earth's core by extrapolation using equations (4.13) and (4.14) when the magnetic fields are strong ($\bar{\Lambda} = O(1)$). We obtain, for molecular diffusivities,

$$R_{\mathrm{c}} = 1.2 \times 10^{16}, \quad L = d = 2 \times 10^6 \text{ m}, \quad T = 4 \times 10^{18} \text{ s}, \quad \text{for } E = 10^{-15}, \tag{4.16}$$

which should be compared with (3.10); and, for turbulent values,

$$R_{\mathrm{c}} = 1.2 \times 10^{11}, \quad L = d = 2 \times 10^6 \text{ m}, \quad T = 4 \times 10^{12} \text{ s}, \quad \text{for } E = 10^{-10}, \tag{4.17}$$

which should be compared with (3.11).

The Rayleigh number required to produce a typical core flow speed of $\mathcal{U} = 10^{-4}\ \mathrm{m\,s^{-1}}$ is

$$R_U = \left[\left|\frac{\mathcal{U}d}{3\lambda}\right|^2 + 12, \right] E^{-1}, \tag{4.18}$$

which gives $R_U = 1.3 \times 10^{18}$ for $E = 10^{-15}$ and 1.3×10^{13} for $E = 10^{-10}$. Both Rayleigh numbers are 100 times critical.

The interpretation of these numbers for the Earth's core is postponed to § 7. We emphasize here the huge contrast between the spatial, temporal and amplitude scales obtained at $\bar{\Lambda} = 0$ (equations (3.10) and (3.11)) and at $\bar{\Lambda} = O(1)$ (equations (4.16) and (4.17)). The smaller the Ekman number, the larger the scale disparities; they are a fundamental characteristic of magnetohydrodynamics in the Earth's fluid core. It is worth noting that these scale disparities are removed almost entirely by hyperviscosity at $E \geqslant 10^{-6}$ (Zhang & Jones 1997): the problem is simply not addressed by the current generation of numerical dynamo simulations employing hyperviscosity.

5. Spatial, temporal and amplitude scales with the effect of a poloidal field

A strong-field dynamo satisfying the Taylor constraint (1.2) is *stable* if small perturbations lead to small changes in the system. Perhaps, intrinsic instability explains why one cannot obtain a strong-field dynamo numerically (see, for example, Fearn & Proctor 1987). We now illustrate a possible instability with two different calculations (linear and nonlinear) with an imposed magnetic field (4.1) that includes a poloidal component ($\epsilon_{\mathrm{P}} \neq 0$).

First, we investigated the linear instability of the magnetoconvective system by including a small poloidal magnetic field while keeping the toroidal field unchanged

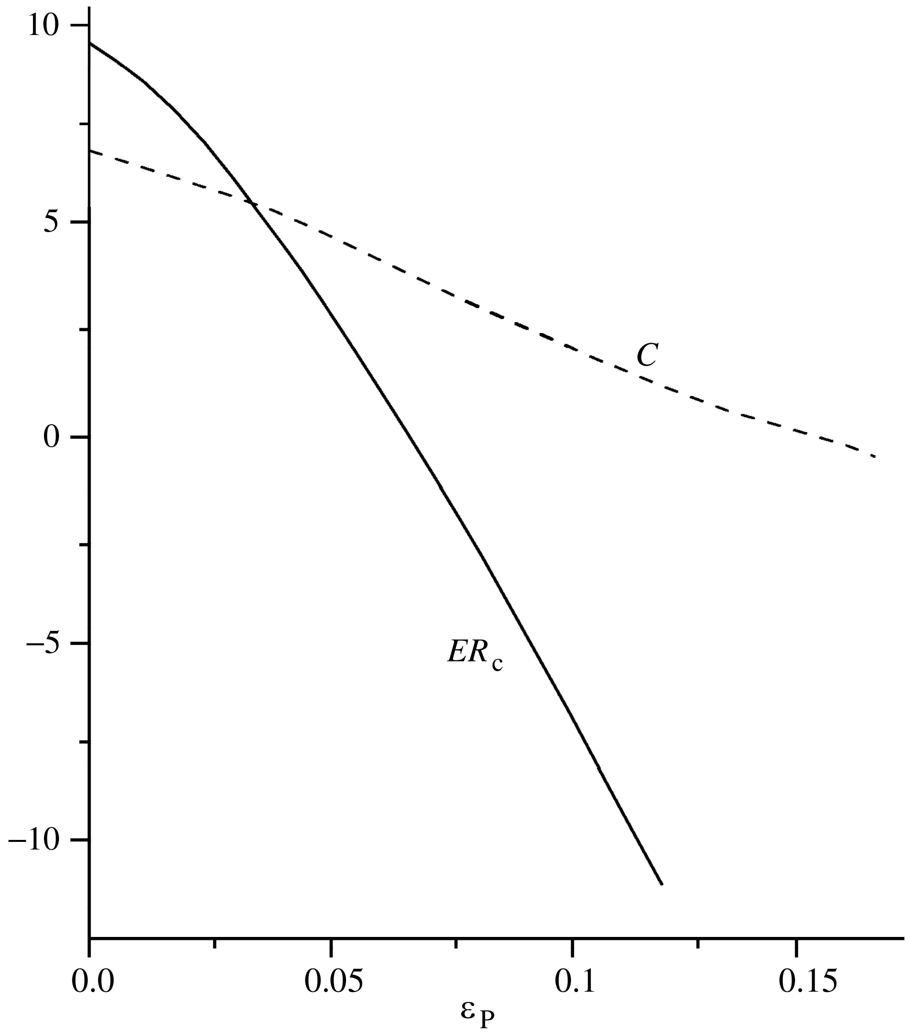

Figure 3. The scaled critical Rayleigh number, ER_c, and the corresponding drift rate C are plotted against ϵ_P at $E = 10^{-4}$. The primary features of this graph are independent of the Ekman number, provided it is small, because of the asymptotic forms (4.13). Reproduced from Zhang & Gubbins (2000) with the permission of Blackwell Science Ltd.

(Zhang & Gubbins 2000). We calculated about 30 solutions at small Ekman number while increasing ϵ_P gradually from zero. We found a dramatic fall in critical Rayleigh number with ϵ_P (figure 3): the product ER_c falls by a factor of 10 as ϵ_P increases from zero to 0.07, still a very small poloidal field. When the Ekman number is very small, this represents a huge fall in R_c itself: a factor of 10^{16} for $E = 10^{-15}$ and 10^{11} for $E = 10^{-10}$. Negative values of R_c correspond to convection driven by the imposed field. Such instabilities could not persist indefinitely for a dynamo-driven field because they draw energy from the imposed field rather than the buoyancy force, but they could be transients in a full dynamo calculation. The point $R_c = 0$ could, therefore, signify an upper bound on the strength of the generated field. The

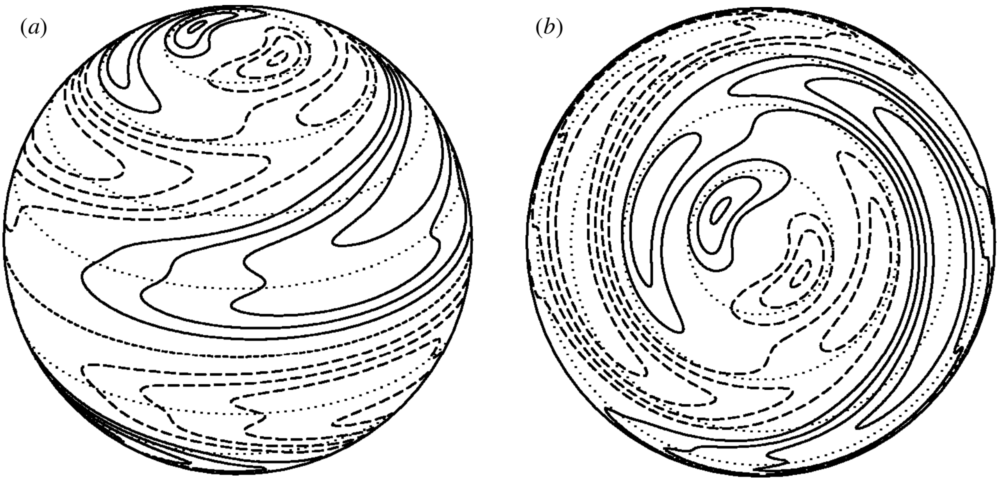

Figure 4. Large spatial scale and long time-scale magnetoconvection at $E = 10^{-5}$ with both toroidal and poloidal magnetic fields imposed: $\Lambda = 10$, $\epsilon_{\mathrm{P}} = 0.017$ (see also table 1). Views (*a*) and (*b*) as in figure 1.

corresponding drift rate of the rolls changes from positive (eastwards) to negative (westwards) as the poloidal field increases. The profile of convection for $\epsilon_{\mathrm{P}} = 0.017$ is shown in figure 4; numerical values are given in table 1.

These results show that linear magnetoconvection can be highly and critically sensitive to small variations in poloidal field when the Ekman number is small. It suggests that the amplitude and pattern of nonlinear convection, which depends on the difference $(R - R_{\mathrm{c}})$ (for example, (4.18)), will change dramatically in response to small variations in poloidal field. This in turn means that the magnetic Reynolds number R_{m} will change dramatically in response to small variations in poloidal field, so that if the field were dynamo-generated rather than imposed we could expect small perturbations in magnetic field to lead to much larger ones, or even a completely different nonlinear solution: typical characteristics of a highly unstable system. We have suggested, on the basis of this result, that a steady convection-driven dynamo will not be stable if the dynamic contribution from the viscous term in equation (1.1) is neglected by enforcing (1.2) (Zhang & Gubbins 2000).

The second analysis is to integrate the fully nonlinear equations (2.5)–(2.7) numerically for fixed Rayleigh number R and toroidal field with and without the poloidal field. It should be noted that the fully nonlinear magnetoconvection solution with both the toroidal and poloidal field is reported here for the first time, but the linear stability calculations have been described in Zhang & Gubbins (2000). A more detailed analysis of the nonlinear problem will be reported in a future paper. The integration always starts from a random initial condition. For $R = 2.2 \times 10^4$, $E = 10^{-3}$, $\epsilon_{\mathrm{P}} = 0$, the final equilibrium solution after a few magnetic diffusion times takes the form of steadily drifting magnetoconvective waves with constant amplitude flow and magnetic field; their phase speed is approximately predicted by linear analysis (C in figure 3; see, for example, Zhang (1999)). The convection is again nearly two-dimensional because of the Proudman–Taylor constraint.

We repeated the calculation with a weak poloidal field ($\epsilon_{\mathrm{P}} = 0.017$), keeping every-

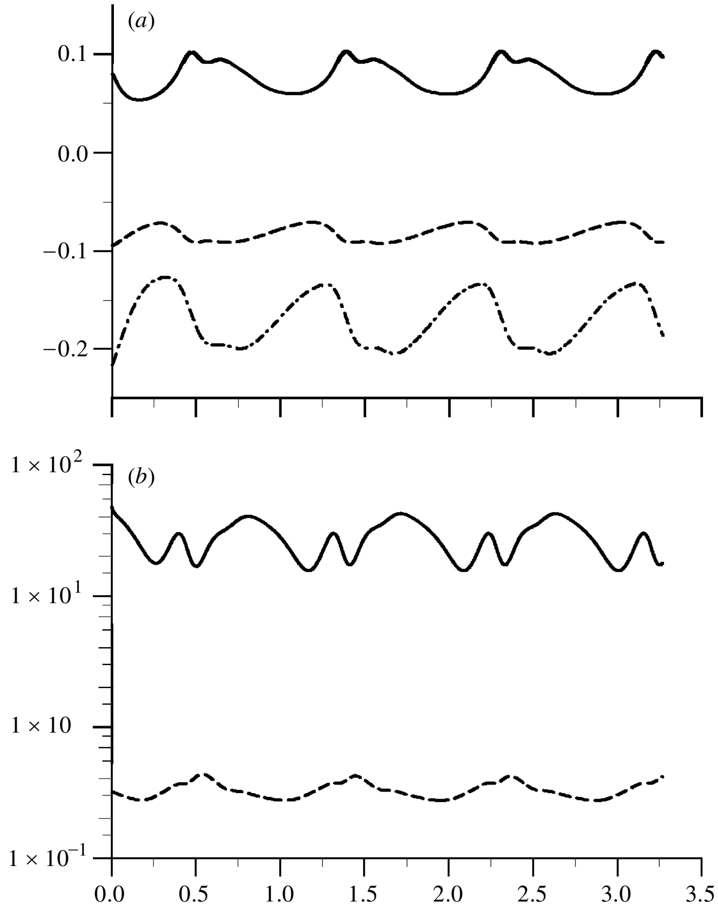

Figure 5. (a) Heat flux at the outer surface (solid line), the leading coefficient of axisymmetric toroidal field (dot-dashed line), and poloidal magnetic field (dashed line) plotted as a function of time for nonlinear magnetoconvection with $R = 2.2 \times 10^4$, $\Lambda = 10$, $\epsilon_{\mathrm{P}} = 0.017$ and $E = 10^{-3}$. (b) Mean toroidal kinetic energy (solid line) and mean poloidal kinetic energy (dashed line) plotted as a function of time for the same solution.

thing else the same. It changed the solution completely; the constant-amplitude travelling wave, which is steady in a corotating frame of reference, is replaced by vacillating magnetoconvection with large-amplitude variations in time. The time variation of the solution is displayed in figure 5, where the kinetic energy of mean toroidal and poloidal convective motions, heat flux and dominant coefficients for the induced axisymmetric toroidal and poloidal magnetic fields are plotted as functions of time.

6. The amplitude of fluid flow required to generate magnetic field

Further evidence of potential instability arises from kinematic studies of the geodynamo in which the fluid flow is fixed, decoupling the induction equation (2.7), which may be solved for $\mathbf{B}$. The problem is linear and, when the flow is steady, presents an eigenvalue problem for the critical magnetic Reynolds number $R_{\mathrm{m}}^{\mathrm{c}}$ with $\mathbf{B}$ as the eigenfunction. The solution for $\mathbf{B}$ can be very highly sensitive to the form of the chosen flow $\mathbf{u}$ (Gubbins *et al.* 2000*a*), often to the extent that dynamo action fails completely after a small change in flow. This result parallels our findings for magnetoconvection to some extent, where the convective flow $\mathbf{u}$ changes dramatically for a small change in applied field $\mathbf{B}$. The nonlinear dynamo, in which the field is self-generated, would, therefore, seem to be subject to a double instability, with small variations in magnetic field producing large changes in flow, and small changes in flow producing large changes in the field.

The kinematic dynamo problem is linear and, therefore, relatively easy to solve numerically, yet there are very few examples of steady flow in a sphere generating magnetic field, and almost no examples of steadily drifting convection acting as a dynamo. This suggests that time dependence of the flow is, perhaps, an important ingredient for dynamo action. To test the efficiency of steady flow in generating magnetic field, Gubbins *et al.* (2000*a*) set up a two-parameter class of fluid motions in a sphere that contained a small number of dynamos first found by Kumar & Roberts (1975) (see also Hutcheson & Gubbins 1994; Sarson & Gubbins 1996) and others found by Love & Gubbins (1996).

The flows comprise large-scale convective rolls with $m = 2$, differential rotation, and meridional circulation:

$$\mathbf{u} = \epsilon_0 \mathbf{t}_1^0 + \epsilon_1 \mathbf{s}_2^0 + \epsilon_2 \mathbf{s}_2^{2\mathrm{c}} + \epsilon_2 \mathbf{s}_2^{2\mathrm{s}}, \tag{6.1}$$

where $\mathbf{t}_l^m$, $\mathbf{s}_l^m$ are toroidal and poloidal vector spherical harmonics,

$$\mathbf{t}_l^{m\mathrm{c,s}} = \nabla \times [t_l^{m\mathrm{c,s}}(r) P_l^m(\sin\theta)[\cos,\sin](m\phi)\mathbf{e}_r], \tag{6.2}$$

$$\mathbf{s}_l^{m\mathrm{c,s}} = \nabla \times \nabla \times [s_l^{m\mathrm{c,s}}(r) P_l^m(\cos\theta)[\cos,\sin](m\phi)\mathbf{e}_r], \tag{6.3}$$

$\mathbf{e}_r$ is the unit vector in the r direction and superscripts 'c' and 's' denote cosine and sine, respectively. The first harmonic in (6.1) represents differential rotation, the second represents meridional circulation, and the last two represent convective overturn. They provide what is thought to be the minimum complexity required to generate a magnetic field possessing the basic features of the Earth's magnetic field and to mimic convection in a rotating sphere.

The scalar functions were chosen to give a $\mathbf{u}$ that is differentiable at the origin, and to be zero with zero stress on the outer boundary:

$$\left.\begin{aligned} t_1^0(r) &= r^2(1-r^2), \\ s_2^0(r) &= r^6(1-r^2)^3, \\ s_2^{2\mathrm{s}}(r) &= r^4(1-r^2)^2\cos(p\pi r), \\ s_2^{2\mathrm{s}}(r) &= r^4(1-r^2)^2\sin(p\pi r). \end{aligned}\right\} \tag{6.4}$$

The flows are parametrized by the fraction of energy in the differential rotation (D), meridional circulation (M), and convection ($C = 1 - |D| - |M|$). Solutions to the induction equation with this flow separate into four symmetries, the dipole and quadrupole solutions referred to in § 3 for convection, and two further solutions characterized by odd azimuthal wavenumbers (the so-called equatorial dipole and quadrupole solutions).

Gubbins *et al.* (2000*a*) found that only 36% of the flows defined by the two parameters D and M generated magnetic fields with dipole symmetry, and that these flows were confined to seven separate zones in (D, M) parameter space. Surprisingly, flows in different zones often generate magnetic fields with similar morphologies. The boundaries of these zones are characterized by small-scale magnetic fields and large critical magnetic Reynolds numbers, where the flow either concentrates the field into very narrow bands producing diffusion, or expels it from the sphere with consequent loss of dynamo generation. Within any zone, it is possible to change the flow parameters considerably without changing the qualitative nature of the dynamo action, yet there are also places where a tiny change in flow will change the solution completely.

In a second study, Gubbins *et al.* (2000*b*) explored other symmetries and found that nearly half of the flows generated fields with at least one symmetry, some could generate two or more symmetries with different $R_{\mathrm{m}}^{\mathrm{c}}$, and some could produce two different symmetries with the same $R_{\mathrm{m}}^{\mathrm{c}}$. This last case delineates a boundary in parameter space that separates physically realizable solutions: on this boundary, an infinitesimal change in flow parameters would change the entire nature of the generated field. Flows with $D > 0$, which correspond to primarily westward flow at the surface of the sphere, generated axial dipole field solutions that were almost exclusively steady. A very small, but perhaps significant, proportion of the flows produced oscillatory solutions.

For some flows, the critical magnetic Reynolds number was found to depend very sensitively on changes in the flow: by a factor of 3 with a 0.1% change in flow and with the appearance of asymptoting to infinity with a finite change in one of the flow parameters (D or M). These rapid changes occurred on the boundaries of zones of dynamo action, and within zones where the steady solution is replaced with an oscillatory solution for a very small interval in M: $-0.010 < M < -0.002$ (Gubbins *et al.* 2000*a*).

These kinematic studies may have implications for the full nonlinear dynamo problem. A time-dependent solution will explore a space of fluid velocities. The observation that the Earth has possessed a non-oscillatory magnetic field with dipole symmetry for most of its history strongly suggests that the flow has a permanent characteristic like the $D > 0$ 'westward drift' of this model. Another observation, that it reverses occasionally, suggests that the flow may occasionally range into a region where another symmetry is generated, or an oscillatory solution is preferred. The third possibility is that the flow takes a form that cannot generate magnetic field, or $R_{\mathrm{m}}^{\mathrm{c}}$ increases dramatically, making dynamo action inefficient. This strong dependence of the dynamo action on the precise form of the flow is a further source of instability in the full nonlinear dynamo.

7. Discussion

This paper was prompted by two developments: the theoretical result that strong-field dynamo models often collapse and lead to non-magnetic convection, and the observation that the geomagnetic field also appears to have suffered frequent collapses in the form of excursions: large departures from the axial dipole form and order-of-magnitude falls in strength. Taken together, these results make it important to understand the stability of the strong-field dynamo in the small-Ekman-number limit, the only model that can explain the geomagnetic field in its present form.

Instability of the strong-field dynamo at small Ekman number presents very major numerical difficulties. We have two choices: either assume the strong-field dynamo is stable and compute solutions at modest Rayleigh number and small Ekman number (but recent calculations suggest this does not work), or resolve the weak-field solution that may develop if the dynamo collapses. The second alternative is safe but impossible for small Ekman number. Our estimates of critical Rayleigh numbers in §§ 3 and 4 differ by a factor of $7E^{-1/3}$ (cf. (3.5) and (4.13)), or 7×10^5 or 3×10^4 depending on whether molecular or eddy diffusivities are used. Starting a strong-field simulation with a Rayleigh number less than several thousand times critical could lead to the convection shutting down completely if the field dropped and R_{c} rose to exceed R. Even with a high value of R, we would have to resolve small length-scales ($m = 70\,000$ or 1600) and, even more seriously, very short time-scales. Such a numerical calculation will remain impossible in the foreseeable future.

Our main hope for understanding the geodynamo must rely on extrapolations of convection-driven dynamo solutions to small Ekman numbers, similar to those in (3.6) and (4.12). We do not yet understand this extrapolation because we do not understand the implications for magnetoconvection when the magnetic field is self-generated: the dynamo instability and its effect on convection has not been studied simply because most convective flows fail to generate a magnetic field. Furthermore, the numerical calculation is intractable even at modest values of the Ekman number. At $E = 10^{-6}$, for example, we would have to resolve wavenumbers out to $m = 200$ (double the expected wavenumber in order to include all primary convective modes) with a time-step $\Delta t < 10^{-6}$ diffusion times in order to resolve the drift frequency of the rolls (10^{-4}). The disparity of scales shown in table 1 explains why all the recent geodynamo models (see, for example, Sarson *et al.* 1998; Olson *et al.* 1999; Katayama *et al.* 1999) have difficulty in reaching $E < 10^{-4}$. It is evident that $E \geqslant 10^{-4}$ is not sufficiently small for the results to be extrapolated to the Earth's core.

A simple way of removing the scale disparities is to introduce hyperviscosity, which is related to the idea of local turbulence and cascades in atmospheric dynamics. There are two objections to the application of hyperviscosity to the Earth's core. The first is the lack of an established turbulent MHD theory. The second, and more important, objection is that the dynamics is fundamentally different from that of the atmosphere. The dynamo problem operates on such a long time-scale that the effect of the inertial term in (2.1), $[\mathbf{u} \cdot \nabla \mathbf{u}]$, is, dynamically, of secondary importance. Regardless of the amplitude of convection, the governing equation of motion is effectively linear when and where the generated magnetic field is weak. In order that convection takes place, the scale of motion must be sufficiently small, as clearly shown by equation (3.1). The dynamic role of viscosity, as explained by Chandrasekhar (1961) (see also Zhang & Busse 1998), is to provide the frictional force necessary to offset the Coriolis force to allow convection. In atmospheric dynamics, or convection in the form of thermal-inertial waves, the inertial term $\mathbf{u} \cdot \nabla \mathbf{u}$ sets up the turbulent energy cascade, and viscosity plays its conventional role of dissipating the smallest length-scales.

Our ideas about the instability are based on magnetoconvection with a constant applied field and kinematic dynamos with constant velocity; we do not know the implications of time-varying applied $\mathbf{B}$ or $\mathbf{u}$ for either case. Indeed, the comparative ease of finding time-dependent dynamos over those with steady flow suggests that time dependence is an important factor, and a time-varying magnetic field may change the nature of magnetoconvection. Both of these problems are under study.

How do we resolve these conflicts of scale? One possible scenario is that a dynamo is neither strong nor weak: it swings between a strong-field dynamo with scaling

(4.13) and a weak-field dynamo with scaling (3.5). Localized small-scale convection with a weak field is ineffective in transporting heat, making it unstable to the dynamo instability, while a strong-field dynamo without viscous effects appears to be unstable because of the high variability of R_c with magnetic field and of R_m^c with fluid flow. Such vacillation between strong- and weak-field states could provide a natural explanation for the repeated falls in field strength observed in the geomagnetic field.

Hollerbach (1997) has already outlined a similar idea, the existence of an intermediate dynamo state (the semi-Taylor state) based on an $\alpha\omega$ dynamo model in a rotating spherical system, which is between the strong- and weak-field states. He suggested that the semi-Taylor state, which describes a temporary departure of the dynamo solutions from the strong-field (Taylor) state and which has a field strength intermediate between the strong- and weak-field dynamos, might be relevant to geomagnetic excursions. The weak-field and semi-Taylor states will be very difficult to distinguish from palaeomagnetic observations because it involves differentiating between a drop in field intensity of perhaps 100 and a drop by a factor of, perhaps, 5. Although palaeomagnetism suggests the fall is by a factor of 5–10 during reversals, temporal averaging and background noise prevent us from measuring any signal that is significantly smaller than this. Furthermore, the dynamics depends mainly on the toroidal field, which is not observable.

Finally, consider now how to apply such a model to the Earth. The present state of the core and geomagnetic field corresponds to a strong-field dynamo, in which the primary force balance is between Coriolis and Lorentz forces. Three quantities should have roughly the right order of magnitude: the convected heat flux; the ohmic heating associated with the generated field; and the magnetic Reynolds number. There is no problem meeting these three requirements with a strong-field dynamo.

Core convection is determined not by an applied Rayleigh number but by the heat flux extracted through the core–mantle boundary as a result of mantle convection, which remains constant on the time-scales of interest for the geodynamo. The heat flux must be greater than that conducted down the adiabatic temperature gradient by the molecular value of the thermal diffusivity; modern estimates place this at about 10^{12} W (Labrosse *et al.* 1997). Any additional heat must be convected by fluid motion.

Sustaining the geomagnetic field by dynamo action driven by thermal convection requires a heat throughput equal to the ohmic heating multiplied by a thermodynamic efficiency factor of about 10 (Backus 1975; Hewitt *et al.* 1975; Gubbins 1977). This result cannot be determined directly from the Boussinesq approximation, which implicitly assumes that the ohmic heating is negligible; it is a more fundamental result and, therefore, a good guide to the heat flux we should expect. If using turbulent diffusivities, we should also consider enhanced viscous and thermally diffusive contributions to the entropy, increasing the heat requirements still further. Compositional convection can reduce the requirements somewhat (Gubbins *et al.* 1979; Loper 1978). These differences are unimportant for the present discussion: the essential requirement is that core convection provides something like 10^{10}–10^{12} W of heat throughput.

The estimate (4.15) for the heat flux from strong-field magnetoconvection yields only 10^8 W. This is too small: it would indeed be amazing if the mantle were to impose a heat flux equal to that required to maintain the adiabat (10^{11} W) plus just an additional 0.1% for the convection! Furthermore, there is a contradiction with the ohmic heating associated with the applied field in the calculation, which is significantly greater than 10^8 W. Most of the energy lost to ohmic heating comes from the (unspecified) source of the applied field; the convection could not, therefore, generate the imposed field by dynamo action, despite the fluid flow being fast enough to give a respectable magnetic Reynolds number.

In a steady dynamo, a simple integral of the induction equation shows that the work done against Lorentz forces is equal to the ohmic heating; in a non-steady dynamo, this balance must be maintained in the time average. In the magnetoconvection calculation there is an imbalance that will lead to decay of the field if the extra source is removed. To model the Earth as it is today we must maintain the same typical flow speed, $\mathcal{U}$, while increasing the Lorentz force. This means a different force balance, and probably a different Rayleigh number. We should not therefore rely on (4.18) as a reliable estimator for the Rayleigh number, although its dependence on E, crucial to the main argument of this paper, remains unaffected.

Now, suppose the field collapses and a weak-field regime, similar to non-magnetic convection, is established. We imagine this weak-field regime corresponds with onset of an excursion, or one of the dips in relative intensity seen in many sediment records (see, for example, Channel, this issue). The weak-field dynamo does not scale to the Earth easily. We have argued that small-scale convection is inefficient at transporting heat, a view sustained by (3.9), which gives only 10^7 W for typical present-day core flow speeds. However, we should not restrict $\mathcal{U}$ to present-day values when the core is in such a dramatically different regime; we should instead adopt the correct heat flux and estimate the resulting flow, which varies as the square root of the heat flux according to (4.15) and (4.18). Raising the heat flux to 10^{11} W increases the flow speed by a factor of 100, to *ca.* $5\ \mathrm{mm\,s^{-1}}$.

Small-scale motions are also inefficient at generating magnetic field. The typical two-scale mechanism (see, for example, Busse 1975) generates field in a two-stage process in which (1) small-scale field $\mathbf{b}^{\mathrm{o}}$ is induced from large scale field $\bar{\mathbf{B}}$ and (2) large-scale field is induced by the average of the action of small-scale flow on small-scale field, $\nabla\times(\overline{\mathbf{u}^{\mathrm{o}}\times\mathbf{b}^{\mathrm{o}}})$. Balancing terms in the dimensionless form of the induction equation, where the large length-scale is $O(1)$, gives

$$R_{\mathrm{m}} = O(l^{-1/2}) \approx 100m^{1/2} = O(E^{-1/6}), \tag{7.1}$$

where the constant factor appearing in (7.1) is justified from calculations for dynamos generating large-scale ($m=1$) magnetic fields, which have $R_{\mathrm{m}}^{\mathrm{c}} \approx 100$. For $E = 10^{-15}$, (7.1) gives $R_{\mathrm{m}} \approx 3\times10^4$, and for $E = 10^{-10}$ it gives $R_{\mathrm{m}} \approx 3\times10^4$, and for $E = 10^{-10}$ it gives $R_{\mathrm{m}} \approx 4000$. The corresponding flow speeds in the core are $0.3\ \mathrm{m\,s^{-1}}$ and $4\ \mathrm{mm\,s^{-1}}$, respectively. Thus, we must have fast core flow to continue to maintain a dynamo when the field is weak.

There remains the problem of satisfying the ohmic heating associated with a small-scale field. Using the same two-scale model as above, the ohmic heating $(\nabla\times\mathbf{b}^{\mathrm{o}})^2$ scales as $R_{\mathrm{m}}^2(\nabla\times\bar{\mathbf{B}})^2$, an increase of a factor of 10^7 for molecular diffusivities and 1600 for turbulent values. $\bar{\mathbf{B}}$ is taken to be one-tenth the size of the present core field in this regime. The molecular value is hard to reconcile: over 10^{13} W. However, the ohmic heating for eddy diffusivities lies within bounds.

In summary, the task of obtaining an Earth-like and self-sustaining numerical geodynamo model remains a major challenge because of the scale disparities associated with an extremely small Ekman number E, which is not only the root of severe difficulties in modelling a convection-driven geodynamo but is also the key feature of the dynamics of the Earth's fluid core.

D.G. was supported by NERC grant GR3/9741. K.Z. is supported by an NERC and a PPARC grant. We thank C. A. Jones and R. Hollerbach for useful discussions.

References

Backus, G. E. 1975 Gross thermodynamic heat engines in deep interior of Earth. *Proc. Natn. Acad. Sci. USA* **72**, 1555–1558.

Busse, F. H. 1970 Thermal instabilities in rotating systems. *J. Fluid Mech.* **44**, 444–460.

Busse, F. H. 1975 A model of the geodynamo. *Geophys. J. R. Astr. Soc.* **42**, 437–459.

Busse, F. H. 1978 Magnetohydrodynamics of the Earth's dynamo. *A. Rev. Fluid Mech.* **10**, 435–462.

Chandrasekhar, S. 1961 *Hydrodynamic and hydromagnetic stability*. Oxford: Clarendon.

Fearn, D. R. 1979 Thermal and magnetic instabilities in a rapidly rotating sphere. *Geophys. Astrophys. Fluid Dyn.* **14**, 103–126.

Fearn, D. R. 1997 The geodynamo. In *Earth's deep interior* (ed. D. Crossley), pp. 79–114. London: Gordon & Breach.

Fearn, D. R. 1998 Hydromagnetic flow in planetary cores. *Rep. Prog. Phys* **61**, 175–235.

Fearn, D. R. & Proctor, M. R. E. 1983 Hydromagnetic waves in a differentially rotating sphere. *J. Fluid Mech.* **128**, 1–20.

Fearn, D. R. & Proctor, M. R. E. 1987 On the computation of steady, self-consistent spherical dynamos. *Geophys. Astrophys. Fluid Dyn.* **38**, 293–325.

Glatzmaier, G. A. & Roberts, P. H. 1995*a* A three-dimensional convective dynamo solution with rotating and finitely conducting inner core and mantle. *Phys. Earth Planet. Interiors* **91**, 63–75.

Glatzmaier, G. A. & Roberts, P. H. 1995*b* A three-dimensional self-consistent computer simulation of a geomagnetic field reversal. *Nature* **377**, 203–208.

Glatzmaier, G. A. & Roberts, P. H. 1996*a* Rotation and magnetism of the Earth's inner core. *Science* **274**, 1887–1891.

Glatzmaier, G. A. & Roberts, P. H. 1996*b* An anelastic evolutionary geodynamo simulation driven by compositional and thermal convection. *Physica* D **97**, 81–94.

Gubbins, D. 1977 Energetics of the Earth's core. *J. Geophys.* **43**, 453–464.

Gubbins, D. 1999 The distinction between geomagnetic excursions and reversals. *Geophys. J. Int.* **137**, F1–F3.

Gubbins, D. & Roberts, P. H. 1987 Magnetohydrodynamics of the Earth's core. In *Geomagnetism* (ed. J. A. Jacobs), vol. II, ch. 1, pp. 1–183. Academic.

Gubbins, D. & Zhang, K. 1993 Symmetry properties of the dynamo equations for paleomagnetism and geomagnetism. *Phys. Earth Planet. Interiors* **75**, 225–241.

Gubbins, D., Masters, T. G. & Jacobs, J. A. 1979 Thermal evolution of the Earth's core. *Geophys. J. R. Astr. Soc.* **59**, 57–99.

Gubbins, D., Barber, C. N., Gibbons, S. & Love, J. J. 2000*a* Kinematic dynamo action in a sphere. I. Effects of differential rotation and meridional circulation. *Proc. R. Soc. Lond.* A **456**. (In the press.)

Gubbins, D., Barber, C. N., Gibbons, S. & Love, J. J. 2000*b* Kinematic dynamo action in a sphere. II. Symmetry selection. *Proc. R. Soc. Lond.* A **456**. (In the press.)

Hewitt, J., McKenzie, D. P. & Weiss, N. O. 1975 Dissipative heating in convective flows. *J. Fluid Mech.* **68**, 721–738.

Hollerbach, R. 1996 On the theory of the geodynamo. *Phys. Earth Planet. Interiors* **98**, 163–185.

Hollerbach, R. 1997 The dynamical balance in semi-Taylor states. *Geophys. Astrophys. Fluid Dyn.* **84**, 85–98.

Hollerbach, R. & Jones, C. A. 1993 Influence of the Earth's inner core on geomagnetic fluctuations and reversals. *Nature* **365**, 541–543.

Hollerbach, R. & Jones, C. A. 1995 On the magnetically stabilizing role of the Earth's inner core. *Phys. Earth Planet. Interiors* **87**, 171–181.

Hutcheson, K. A. & Gubbins, D. 1994 Kinematic magnetic field morphology at the core mantle boundary. *Geophys. J. Int.* **116**, 304–320.

Jault, D. 1995 Model Z computation and Taylor's condition. *Geophys. Astrophys. Fluid Dyn.* **79**, 99–124.

Jones, C. A., Longbottom, A. W. & Hollerbach, R. 1995 A self-consistent convection driven geodynamo model, using a mean field approximation. *Phys. Earth Planet. Interiors* **92**, 119–141.

Jones, C. A., Soward, A. M. & Mussa, A. I. 2000 The onset of thermal convection in a rapidly rotating sphere. *J. Fluid Mech.* **405**, 157–179.

Katayama, J. S., Matsushima, J. S. M. & Honkura, Y. 1999 Some characteristics of magnetic field behavior in a model of MHD dynamo thermally driven in a rotating spherical shell. *Phys. Earth Planet. Interiors* **111**, 141–159.

Kuang, W. & Bloxham, J. 1997 An Earth-like numerical dynamo model. *Nature* **389**, 371–374.

Kumar, S. & Roberts, P. H. 1975 A three-dimensional kinematic dynamo. *Proc. R. Soc. Lond.* A **344**, 235–238.

Labrosse, S., Poirier, J.-P. & LeMouël, J.-L. 1997 On cooling of the Earth's core. *Phys. Earth Planet. Interiors* **99**, 1–17.

Loper, D. E. 1978 Some thermal consequences of a gravitationally powered dynamo. *J. Geophys. Res.* **83**, 5961–5970.

Love, J. & Gubbins, D. 1996 Dynamos driven by poloidal flows exist. *Geophys. Res. Lett.* **23**, 857–860.

Moffatt, H. K. 1978 *Magnetic field generation in electrically conducting fluids*. Cambridge University Press.

Olson, P. & Glatzmaier, G. 1995 Magnetoconvection in a rotating spherical shell: structure of flow in the outer core. *Phys. Earth Planet. Interiors* **92**, 109–118.

Olson, P. & Glatzmaier, G. 1996 Magnetoconvection and thermal coupling of the Earth's core and mantle. *Phil. Trans. R. Soc. Lond.* A **354**, 1–12.

Olson, P., Christensen, U. & Glatzmaier, G. 1999 Numerical modeling of the geodynamo: mechanisms of field generation and equilibration. *J. Geophys. Res.* **104**, 10 383–10 404.

Proctor, M. R. E. 1994 Magnetoconvection in a rapidly rotating sphere. In *Stellar and planetary dynamos* (ed. M. R. E. Proctor & A. D. Gilbert). Cambridge University Press.

Roberts, P. H. 1965 On the thermal instability of a highly rotating fluid sphere. *Astrophys. J.* **141**, 240–250.

Roberts, P. H. 1968 On the thermal instability of a self-gravitating fluid sphere containing heat sources. *Phil. Trans. R. Soc. Lond.* A **263**, 93–117.

Roberts, P. H. & Soward, A. M. 1992 Dynamo theory. *A. Rev. Fluid Dyn.* **24**, 459–512.

Sarson, G. & Gubbins, D. 1996 Three-dimensional kinematic dynamos dominated by strong differential rotation. *J. Fluid Mech.* **306**, 223–265.

Sarson, G. R. & Jones, C. A. 1999 A convection driven geodynamo reversal model. *Phys. Earth Planet. Interiors* **111**, 3–20.

Sarson, G. R., Jones, C. A. & Longbottom, A. W. 1998 Convection driven geodynamo models of varying Ekman number. *Geophys. Astrophys. Fluid Dyn.* **88**, 225–259.

Soward, A. M. 1977 On the finite amplitude thermal instability of a rapidly rotating fluid sphere. *Geophys. Astrophys. Fluid Dyn.* **9**, 19–74.

Taylor, J. B. 1963 The magneto-hydrodynamics of a rotating fluid and the earth's dynamo problem. *Proc. R. Soc. Lond.* A **274**, 274–283.

Walker, M. R. & Hollerbach, R. 1999 The adjustment to Taylor's constraint in the presence of an ambient field. *Phys. Earth Planet. Interiors* **114**, 181–196.

Walker, M. R., Barenghi, C. F. & Jones, C. A. 1998 A note on dynamo action at asymptotically small Ekman number. *Geophys. Astrophys. Fluid Dyn.* **88**, 261–275.

Zhang, K. 1991 Convection in a rapidly rotating spherical fluid shell at infinite Prandtl number: steadily drifting rolls. *Phys. Earth Planet. Interiors* **68**, 156–169.

Zhang, K. 1992 Spiralling columnar convection in rapidly rotating spherical fluid shells. *J. Fluid Mech.* **236**, 535–556.

Zhang, K. 1994 On coupling between the Poincaré equation and the heat equation. *J. Fluid Mech.* **268**, 211–229.

Zhang, K. 1995*a* Spherical shell rotating convection in the presence of a toroidal magnetic field. *Proc. R. Soc. Lond.* A **448**, 245–268.

Zhang, K. 1995*b* On coupling between the Poincaré equation and the heat equation: non-slip boundary condition. *J. Fluid Mech.* **284**, 239–256.

Zhang, K. 1999 Nonlinear magnetohydrodynamic convective flows in the Earth's fluid core. *Phys. Earth Planet. Interiors* **111**, 93–105.

Zhang, K. & Gubbins, D. 2000 Is the geodynamo process intrinsically unstable? *Geophys. J. Int.* **140**, F1–F4.

Zhang, K. & Jones, C. A. 1993 The influence of Ekman boundary layers on rotating convection. *Geophys. Astrophys. Fluid Dyn.* **71**, 145–162.

Zhang, K. & Jones, C. A. 1994 Convective motions in the Earth's fluid core. *Geophys. Res. Lett.* **21**, 1939–1942.

Zhang, K. & Jones, C. A. 1997 The effect of hyperviscosity on geodynamo models. *Geophys. Res. Lett.* **24**, 2869–2872.

Zhang, K.-K. & Busse, F. H. 1998 Some recent developments in the theory of convection in rotating systems. *Adv. Fluid Mech.* **20**, 17–70.